

VALORIZATION OF ALGERIAN MARINE
Dictyopteris polypodioides BIOMASS IN THE DESIGN OF
 BIOMATERIALS FOR FOOD PACKAGING

CHADIA IHAMOUCHEM, NADIA AOUDIA, HOCINE DJIDJELLI and AMAR BOUKERROU

*Laboratory of Advanced Polymer Materials, Faculty of Technology,
 University of Bejaia, 06000 Bejaia, Algeria*

✉ *Corresponding author: C. Ihamouchen, ihchadou@yahoo.fr*

Received December 16, 2019

Efficacious waste utilization is vital in the context of sustainability. The main objective of this work is to valorize marine biomass by extracting sodium alginate from the brown algae of *Dictyopteris polypodioides* species and to develop a new material based on a biodegradable polymer, *i.e.* polylactic acid (PLA). Films were prepared based on PLA and sodium alginate powder (10, 20 and 30% by weight) and glycerol was incorporated as a plasticizer. The yield of sodium alginate was estimated at 30%. FTIR spectra of *Dictyopteris polypodioides* confirmed the high uronic acid content and XRD analyses proved the amorphous nature of the alginate. Adding alginate to the PLA matrix produced an increase in water vapor permeability values and led to interactions between PLA and alginate. No antibacterial activity was detected in our products against the two bacterial strains tested (*Staphylococcus aureus*, *Pseudomonas*), nor against the *Botrytis* fungus. The films with 10 and 20% sodium alginate exhibited an inhibitory effect on the *Penicillium* fungus.

Keywords: brown seaweed, *Dictyopteris polypodioides*, sodium alginate, viscosity, FTIR spectroscopy

INTRODUCTION

Plastics are in high demand, particularly in regular and take-away food packaging. Despite their many advantages, synthetic polymers present real drawbacks, conducing to the production of large volumes of waste and to the decrease of oil and gas reserves, as well as to environmental concerns caused by their degradation and to toxicity risks to consumers, including the migration of monomers, oligomers or additives to edible substances.¹ This is the reason why many initiatives are undertaken around the world to reduce their ecological impact and to develop substances of biotechnical interest from natural and renewable resources. Biopolymers, such as starch, gluten and guar gum, are suitable alternatives to make packaging materials, due to their non-toxicity, biodegradability, and synthesis from renewable resources.

In the vast ocean realm, several forms of life (from unicellular to multicellular organisms) flourish and multiply. Marine living resources, such as seaweeds, could be termed the promising

plants of the future. Although oceans and seas represent nearly three-quarters (71%) of the Earth's surface, the exploitation of marine biomass has been largely disregarded and therefore not been used judiciously enough, unlike their terrestrial analogues. About 90% of the species of marine plants are algae and about 50% of the global photosynthesis is algae-derived. Thus, every second, several molecules of oxygen we inhale come from algae and algae re-use every second several molecules of carbon dioxide we exhale.²

Algae are known as living chlorophyll photosynthetic organisms found in aquatic environments. There are two main categories of algae: micro-algae (unicellular) and macro-algae (multicellular).³ The importance of seaweeds for human consumption has been well known since 300 BC by the Chinese and Japanese, who are the major world seaweed cultivators, producers and consumers.⁴ According to statistics from the FAO (Food and Agriculture Organization of the United Nations), the world total seaweed production in

2014 was 28.5 million tons: with an increase of 94% in 10 years to meet the ever-increasing food demand no longer met by harvesting.⁵ Algae aquaculture has tremendously developed. It is now a major economic development issue.

The main substances extracted from algae are polysaccharides, referred to as phycocolloids, such as agars, carrageenans and alginates. Alginates are naturally present as salts in the cell walls of brown algae. They are complex polysaccharides composed of two uronic acids: β -D-mannuronic acid (M) and α -L-guluronic acid (G), arranged either in heteropolymeric (MG) or in homopolymeric (MM or GG) blocks.⁶ The M/G ratio and block structure has a major impact on the physico-chemical properties of alginates. Typically, by rising the guluronic acid (G) content or molecular weight, rigid and brittle alginate gels may be achieved. Inversely, more flexible gels may form due to a high amount of alginate-M blocks.⁷ The proportion of one to the other determines the gelling characteristics of the product.

Seaweeds are sold in a dried or fresh form as a vegetable; they generally contain proteins, minerals, and vitamins. They are industrialized under the reference E400. They allow giving the desired texture to most of the aqueous solutions we commonly use, without changing their flavor, color or shape. Their applications are numerous and diverse. Alginate is an excellent stabilizing and thickening agent used in foods, such as drinks, jelly, ice-cream, desserts. It can serve as a good material in dental impression, due to its thermo-reversible properties, hydrophilicity, pleasant odor and taste, ease of mixing and low cost.⁸ Commercially, there are alginate based wound dressings, which can accelerate wound healing, compared with control dressings, due to the presence of endotoxin in alginate.⁹ Studies revealed that the reconstruction and regeneration of rat peripheral nerve gap can be performed without sutures and with a tubular structure using only alginate gels.^{10,11} Studies concluded that the combination of modified citrus pectin (MCP)/alginate can reduce an average of 74% of toxic heavy metals in the body, without any side effects.¹² Recently, in tissue engineering, alginate has also been utilized as a 3D platform for microarray systems, as well as surface micro-patterning.¹³ The adsorption and degradation capacity towards organic compounds of zero-valent iron nanoparticles entrapped in calcium alginate beads was evaluated by Kexin Yi *et al.*¹⁴

The experimental results showed that the free calcium ions contained in Ca-alginate had a significant impact on the adsorption and degradation behaviors of positively charged pollutants, but those of neutrally and negatively charged pollutants were only moderately affected. B. Wang *et al.*¹⁵ studied the thermal degradation properties, flammability, and flame-retardant mechanism of bio-based cotton/alginate blends. The alginate fibers improved the thermal degradation properties, enhanced the flame-retardant properties and fire behaviors, and decreased the peak heat release rate, total smoke production, CO₂ production, and the released amount of inflammable volatiles. The flame retardant properties of cotton/alginate blended fibers can meet the requirements for filling materials for indoor furniture, such as toys, sleeping bags and pillows. *Zymomonas mobilis* strain immobilized in doped calcium alginate (Ca-alginate) threads was successfully employed for the production of ethanol by Akira Nordmeier *et al.*¹⁶

The exploitation of the Algerian marine environment could be of great interest, since Algeria has a maritime coast stretching over 1200 km. The study of the algal flora of Algeria has been the subject of several studies.¹⁷ However, these algological studies are essentially of the inventory type, and chemical contributions that have focused on the extraction and purification of alginates are very rare. It is for this reason that this work has been carried out with two objectives: the first is to valorize marine biomass by extracting sodium alginate from brown algae of the *Dictyopterus polypodioides* species and the second is to develop a new material based on an algal extract (alginate) and on a biodegradable polymer (PLA) for food packaging applications.

EXPERIMENTAL

Materials

The poly(lactic acid) used in this study was supplied in granular form by Nature Works; it is referred to by its industrial reference "7001D". Its main characteristics are as follows: density – 1.24, melt flow index (210 °C, 2.16 Kg) – 6 g/10 min, melting temperature – 145-160 °C and weight average molecular weight M_w equal to 113000 g/mol.

Brown algae, corresponding to the species *Dictyopterus polypodioides* (Fig. 1), were collected during February from the coasts of Saket, Bejaia city (Algeria). They were first washed with seawater and then transported directly to the laboratory in plastic bags. Once in the laboratory, the algae were manually

sorted to eliminate any source of contamination (larvae, crustaceans, sand *etc.*), washed successively with tap water and rinsed with distilled water. The fresh algae were preserved for later use.

Two bacterial strains were used: a gram-positive one (*Staphylococcus aureus* (6726TSB)) and a gram-negative one (*Pseudomonas* (ATCC 29522)), as well as two types of fungi: *Botrytis* and *Penicillium*. These strains were provided by the Microbiology Laboratory of the University of Bejaia.

Extraction of sodium alginate

The extraction protocol is similar to that of Torres *et al.*,¹⁸ with some modifications. A certain amount of fresh, carefully washed seaweed was cut into 2 to 3 mm particles and then rehydrated in a 2% formaldehyde solution for 24 hours at room temperature. The purpose of this operation is to avoid microbial contamination and to stabilize the phenols that would oxidize in the next step. The residual biomass was filtered, washed with distilled water, and collected. Then, it was immersed in a solution of sulphuric acid H₂SO₄ at 0.2 N for demineralization for at least one night. Several rinses with distilled water are necessary. The washing water carries with it the mineral salts and some of the pigments. The fresh seaweed mass recovered after filtration was placed in a beaker. Dry weight measurement was carried out in parallel to determine the percentage dry weight of the algae for yield calculation. Thus, the biomass was suspended in 4% Na₂CO₃ solution at room temperature, and the extraction lasted for 10 h. Sodium alginate was collected by filtration and precipitated with 95% absolute ethanol (1:2 v/v). Once precipitated, the mass thus obtained was washed with acetone, allowing it to be bleached, dried in an oven at 60 °C for 48 hours and then finely ground to a powder form.

Formulations

Different formulations were developed, namely: an initial formulation with 100% PLA noted as F0, and three formulations based on PLA and sodium alginate in different ratios (5, 10 and 20% by weight), noted as F5SA, F10SA and F20SA, respectively.

Film preparation

The preparation of the films in solution was carried out according to a method developed in our laboratory: 1 g of each formulation (total mass of the mixture) was weighed. The PLA solution was prepared by dissolving the PLA matrix separately in 25 mL of chloroform at room temperature, stirring until complete dissolution (about 30 min). In parallel, the same was done for sodium alginate, but in 20 mL of distilled water and under stirring until complete dissolution. Once dissolved, the two solutions were mixed, and then 1 mL of glycerol was added to the mixture as plasticizer. Note that emulsifier (Tween 80) was used in the preparation of the emulsions.

Specifically, the following protocol of emulsification was followed. First, appropriate volumes of alginate and PLA were transferred into a vial. The solution was then homogenized using a vortex mixer to obtain a pre-emulsion. The pre-emulsion was ultrasonically processed for 1 min. When the mixture became homogeneous, it was cast onto Petri dishes (90 mm in diameter), using the same volumes of films, and allowed to dry for 24 h, at room temperature and 40-50% relative humidity (RH). The schematic representation of the emulsification process is shown in Figure 2.

Characterization

Alginate yield

The crude alginate yield was calculated according to the following Equation (1):

$$\text{Alginate yield (\%)} = \frac{M_{SA}}{M_{algae}} \times 100 \quad (1)$$

where the weight of dry algae used for extraction is M_(algae) and the mass of the dry extract (sodium alginate) is M_(SA).

Molecular weight

The viscosity average molecular weight (M_w) of alginate samples was determined by capillary viscometry at 25 °C, using an Ubbelohde Capillary Viscometer. Alginate dilute solutions were prepared in 0.1 M of NaCl. The intrinsic viscosity [η] was measured by the intercept of the Huggins plot (reduced viscosity as a function of concentration) when the concentration was zero. M_w was calculated by the Mark-Houwink-Sakurada equation (2):¹⁹

$$[\eta] = K_v \cdot M_w^a \quad (2)$$

where [η]: intrinsic viscosity (L. g⁻¹), K_v, a: characteristic parameters of the polymer/solvent system at a given temperature and M_w: viscosity average molecular weight (g.mol⁻¹). The K_v and a were estimated according to Vold *et al.*²⁰ (K_v = 0.00504 and a = 1.01).

FTIR analysis

FTIR spectra of the samples were recorded with a Shimadzu FTIR-8400 S spectrometer in the absorbance mode. The samples were scanned from 4000 to 400 cm⁻¹, with 32 scans recorded at 4 cm⁻¹ resolution. Alginates were mixed with KBr.

X-ray diffraction (XRD)

X-ray diffraction (XRD) measurements of the alginate film and of the composite films were carried out on an XPert Pro Panalytical diffractometer, using Cu-Kα radiation (λ = 1.540598 Å) over a 2θ range of 2-70° with a step size of 0.016.

The degree of crystallinity was calculated from the ratio of the crystalline phase to the total area, according to the following equation, the values of which were obtained by the "X'Pert High Score" software:

$$X_c \% = \frac{A_c}{A_c + A_a} \times 100 \quad (3)$$

where X_c : the degree of crystallinity, A_c : the area of the crystalline phase, A_a : the area of the amorphous phase.

Thermal analysis

The thermal stability of the samples was determined with a Seteram TG/DTA92 thermal analyzer. The TGA profile was recorded over a temperature range from room temperature to 600 °C, at the heating rate of 10 °C/min in a nitrogen atmosphere.

Water vapor permeability

Water vapor permeability (WVP) of the samples was determined using the gravimetric method, by taking advantage of the absorbent properties of calcium carbonate, according to NF XP H00-313 standard. For each film, a bag sample (50 x 50 mm) was prepared, which was filled with 50 g of dehydrated CaCO₃ before being sealed. The sealed bags were placed into a water bath heated to 40 ± 2 °C, at a humidity level of about 90%, so that no part of the



Figure 1: Raw material – algae

Antimicrobial and antifungal activity

The antimicrobial activities of the films were investigated using the agar disc diffusion method. Sterile discs of the tested films of 6 mm in diameter (sterilization for 15 min in a UV hood) were prepared. Sterile Muller Hinton agar was poured into Petri dishes, with a thickness of 2 mm, and uniformly distributed. The Petri dishes were dried for 30 min at room temperature and then seeded to ensure a homogeneous distribution of bacteria (*Staphylococcus aureus* (6726TSB) and *Pseudomonas* (ATCC 29522)). Using sterile forceps, the film discs to be tested were deposited on the surface of the inoculated agar. Antibacterial activity was determined in terms of the diameter of the inhibition zone produced around the discs after 24 hours of incubation at 37 °C. The same procedure and steps were followed for the antifungal test, the fungi tested were *Botrytis* and *Penicillium*, and the incubation was performed at 25 °C for 48 hours.

bags was immersed. The principle of this test is to quantify the amount of water absorbed by the calcium carbonate for 24 hours. After about 24 hours, the bags were opened and the calcium carbonate contained in each bag was weighed. The calcium carbonate was then dried in an oven at 40 °C for 48 hours before being weighed again. All the results represent an average value obtained from three tests performed.

Finally, the water vapor permeability rate (WVPR) and the water vapor permeability (WVP) were calculated using the following equations:

$$WVPR (g/m^2 \cdot days) = \frac{\Delta m}{\Delta t \cdot A} \quad (4)$$

$$WVP (g \cdot m/m^2 \cdot days \cdot Pa) = \frac{WVPR \cdot e}{\Delta P} \quad (5)$$

where $\Delta m/\Delta t$ is the rate of moisture gain, (g/h), A : the exposed area of the film (m²), e : thickness, (m); and ΔP is the difference in partial water vapor pressure between the two sides of the film specimens.

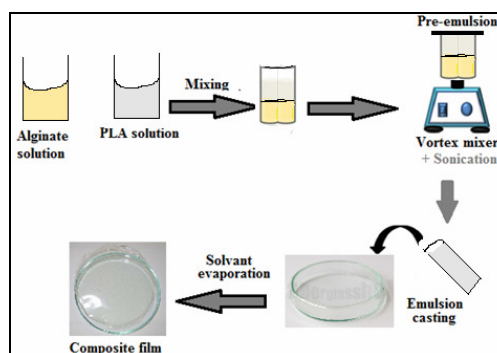


Figure 2: Protocol of emulsification and homogenization

RESULTS AND DISCUSSION

Characterization of sodium alginate

Alginate yield

The sodium alginate yield for the species *Dictyopterus polypodioides* is about 30% PS (% sodium alginate based on the dry weight initially used). In comparison with the data reported in the literature^{21,22} (Table 1), the alginate content of the species *Dictyopterus polypodioides* is very promising and similar to those of some alginophytes, such as *Laminaria digitata* (22-36% PS), *Laminaria hyperborea* (24-33% PS). However, this level remains lower than those of alginophytes that dominate the global alginate industry market, such as *Durvillaea antarctica* (53% PS) and *Ecklonia cava* (35-38% PS). This variation can be explained by several factors that

influence the biochemical composition of the algae, such as the part of the thallus used, the age of the thallus, the harvesting site, the season, the concentration of the sodium carbonate solution and the extraction time. Studies have shown that

intrinsic factors, such as geographical and climatic factors, genetic factors, the degree of maturity of the plant and the storage time have a strong influence on this yield value.²³

Table 1
Alginate content in the species studied and in other alginophytes

Species	Alginate content (% dry weight)
<i>Laminaria japonica</i>	20-26
<i>Laminaria hyperborea</i>	24-30
<i>Laminaria digitata</i>	22-36
<i>Ecklonia cava</i>	35-38
<i>Durvillaea antarctica</i>	53
<i>Lessonia trabeculata</i>	25.67
<i>Dictyopteris polypodioides</i>	30 (This study)

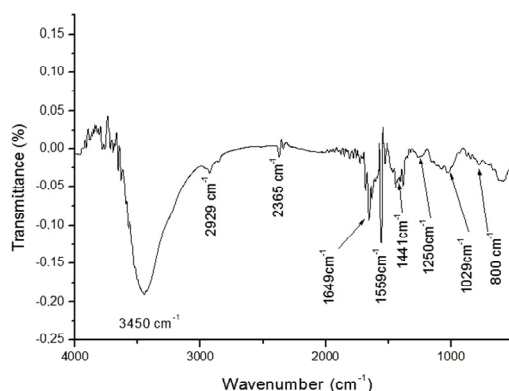


Figure 3: FTIR spectrum of sodium alginate

FT-IR analysis

The FTIR spectra of sodium alginate isolated from *Dictyopteris polypodioides* are shown in Figure 3. According to the bibliography, several authors have already identified the characteristic bands of sodium alginate. Among them, the following have been distinguished:

- A wide band at 3450 cm⁻¹, which corresponds to the elongation of the O-H group, and a band at 2929 cm⁻¹, which can be attributed to the elongation of the C-H group;
- Another characteristic band appears at 1649 cm⁻¹ and is attributed to the asymmetric elongation of the carboxylate group COO, confirming the high uronic acid content of the polysaccharide;²⁴
- A weak band located around 1559 cm⁻¹ corresponding to the vibrations of the C=C elongations;
- A band located around 1442 cm⁻¹ corresponding to the vibrations of O-H deformations, with the contribution of the

symmetrical stretching of the carboxylate group COO;²⁵

- A band located around 1254 cm⁻¹ corresponding to the vibrations of C-C-O elongations;
- A band located around 1022 cm⁻¹ corresponding to the -C-O valence vibrations;

The region between 850-600 cm⁻¹ has been widely discussed by Silverstein *et al.* and Mathlouthi and Koenig.^{25,26} According to these authors, the very weak band at 850 cm⁻¹ is characteristic of a cyclic compound that has been assigned to the C-O vibration stretching of uronic acid residues, and the one at 800 cm⁻¹ is assigned to the C-H deformation vibration of α -L-guluronic acid residues.

Determination of molecular weight by viscometry

The molecular weight was calculated from the equation HMS (Houwink-Mark-Sakurada),

linking the intrinsic viscosity to the mass average molecular weight: $[\eta] = K \cdot M_w^a$.

The parameters “a” and “K” depend on the nature of the solvent and the polymer. In the specific case of alginates solubilized in water, the characteristic parameters of the relationship described by Vold²⁰ are used:

$$[\eta] = 0.00504 M_w^{1.01}$$

A linear regression of the reduced viscosity plot as a function of concentration gives the value of the ordinate at the origin, corresponding to the intrinsic viscosity $[\eta]$, the approximation is acceptable for low concentration values. The intrinsic viscosity and average molecular weight values are presented in Table 2.

X-ray diffraction

Table 2
Intrinsic viscosity and average molecular weight of sodium alginate

Sample	$[\eta]$ (dL/g)	M (g/mole)
Sodium alginate	0.668	117 931.48

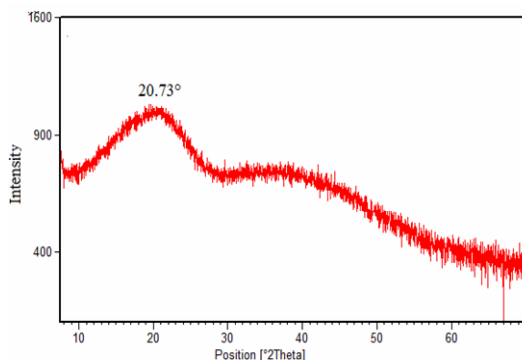


Figure 4: X-ray diffractogram of sodium alginate

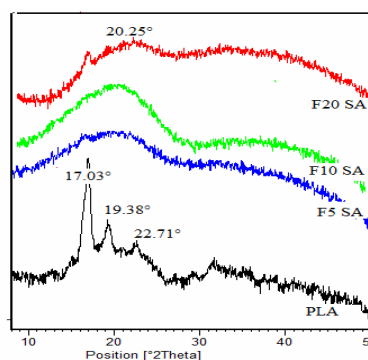


Figure 5: X-ray diffractograms of PLA/alginate films

Characterization of PLA/SA films

X-ray diffraction

XRD diffractograms of PLA/alginate films are shown in Figure 5. According to Figure 5, the PLA diffraction pattern shows an intense peak with a maximum at 17.03° and two other low intensity peaks located at 19.38° and 22.71°, indicating its semi-crystalline state. These results are in perfect agreement with other previous studies, where the XRD pattern of pure PLA has been described by Mihai *et al.*³⁰ and R. Nasrin *et al.*³¹ They observed the presence of the three peaks described above around 16.50°, 19° and 22.3°.

The addition of 20% sodium alginate to the PLA matrix allows the intensity of the first peak to decrease; the gradual reduction in intensity is

Figure 4 shows the XRD pattern of sodium alginate. Alginate powder has a wide peak in the 15° to 24° range, with a central position at $2\theta = 20.73^\circ$, characteristic of the alginate structure and corresponding to the amorphous region of the alginate. In comparison with the results reported in the literature and according to Paşcalău *et al.*,²⁷ for an unplasticized alginate film, this peak is sharper due to the likely rearrangement of alginate chains. This phenomenon has also been observed in the case of plasticized chitosan.²⁸ In other words, the more the amount of the plasticizer (glycerol) increases, the more the intensity of the peak decreases, indicating a larger proportion of the amorphous structure.²⁹

caused by the difference in relative crystallinity between PLA and sodium alginate as already described above. On the other hand, for lower alginate ratios (5 and 10%), the peaks are transformed into a very wide shoulder centered at 20.25°, characteristic of the alginate structure and corresponding to its amorphous form. In addition, the PLA/alginate diffraction peaks at 19.38° and 22.71° have disappeared, suggesting that the regular crystal structure has been disrupted by the hydrogen bonds and the electrostatic interaction established between alginate and PLA.³² In addition, the latter is fully dissolved and dispersed in the amorphous phase of sodium alginate, regardless of the loading ratio, which leads to the existence of a low broad peak centered at 19°.

The X-ray diffraction method allows us to determine the crystallinity degree of the films prepared with sodium alginate using appropriate software, following Equation (3). The results obtained are summarized in Table 3. From the results of the table, it can be seen that the crystallinity degree of neat PLA is 44%, a much higher value than that of the various PLA/alginate films, because it is suggested that the alginate reacts first in the amorphous regions (better accessibility) of the PLA matrix. On the other hand, the difficulties will be more important for the crystalline regions with compact and ordered structure, and then alginate reacts at the end of the

chains or on the surface of the crystallites, causing the chains linked by hydrogen bonds to open, thus promoting the formation of the amorphous phase. For charged films, the degree of crystallinity increases with the increase in the charge, hence these charges play the role of a nucleating agent, which accelerates the crystallization process.

Thermogravimetric analysis (TGA)

Thermogravimetric analysis was performed to study the thermal stability of the prepared films. The TG and DTG curves for PLA, sodium alginate and the films loaded with 5 and 20% filler are shown in Figures 6 and 7.

Table 3
Crystallinity degree of PLA/alginate films

Formulation	F0 (neat PLA)	F5 SA	F10 SA	F20 SA
Crystallinity degree (%)	44	0.44	0.97	2.48

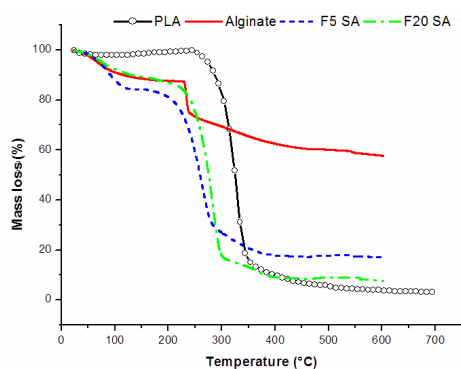


Figure 6: TG thermograms of PLA/alginate films (circle: neat PLA, solid line: alginate, dashed line: F5 SA and dash dotted line: F20 SA)

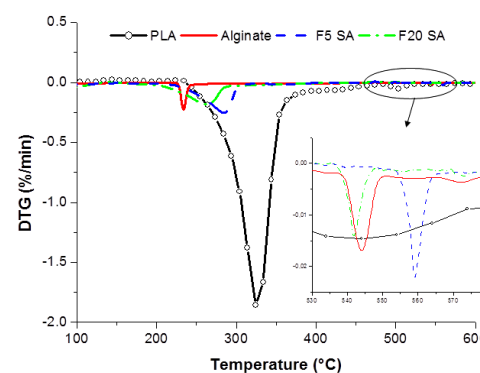


Figure 7: DTG thermograms of PLA/alginate films (circle: neat PLA, solid line: alginate, dashed line: F5 SA and dash dotted line: F20 SA)

Table 4
Results of water vapor permeability

Samples	Thickness (m)	WVPR (g/m ² .h)	WVP (g.m/m ² .h.Pa)
F0 (PLA)	1.5×10^{-3}	15.32	1.44×10^{-6}
Alginate	1.3×10^{-3}	36.42	15.78×10^{-6}
F5 SA	1.3×10^{-3}	11.25	4.87×10^{-6}
F10 SA	1.2×10^{-3}	13.34	5.33×10^{-6}
F20 SA	1.3×10^{-3}	14.67	6.35×10^{-6}

On the TGA thermogram of PLA, the first degradation step is recorded ranging from 25 °C to 230 °C, where the sample is thermally stable. From the estimated initial decomposition temperature of 250 °C, PLA undergoes a very significant mass loss estimated at more than 92%, which is attributed to its depolymerization or to

the decomposition of PLA chains. Above 265 °C, the third degradation stage is recorded and it corresponds to the formation of the residue.

The thermogram of alginate powder exhibits three degradation steps. The first stage of weight loss, between 50 and 200 °C, is mainly caused by the evaporation of water absorbed on the surface

of the alginate powder and by the breaking of glycosidic bonds.³³ The second step ranges between 250 °C and 450 °C, corresponding to the thermal decomposition of alginate. At this stage, the alginate powder shows a sharp peak in the DTG curve, which could be attributed to the partial overlap of the different degradation processes, such as the further breakdown of glycosidic bonds, and the dehydration of saccharide cycles resulting in the formation of intermediate material. The degradation leaves about 58% of alginate residue at 600 °C. The third weight loss of the alginate between 550 and 600 °C is observed only on the DTG thermograms (magnified area). This step is due to the degradation of the fragments formed in the second step caused by the oxidation of the carbonaceous residues.³⁴

The loaded samples have a significantly lower initial decomposition temperature and mass losses (5% and 50%) than the corresponding values of the PLA matrix. The maximum decomposition rate decreases with the incorporation of alginate and decreases further with the increase in the loading ratio, estimated at 0.23, 0.26 and 2.12%/min for F20, F5 and PLA films, respectively. There is also a shift in maximum decomposition temperatures towards lower values, signaling a decrease in the thermal stability of alginate films, compared to the PLA matrix. It should also be noted that the analysis (TG) also indicates that the PLA/alginate films generate more residue. Similar results have been observed previously,³⁵ indicating that thermal degradation accelerated in the presence of alginate.

Water vapor permeability

The WVP of a film is an essential parameter for its application in food packaging, since it must lower the water permeation from the outside environment to the inside of the package. It is dependent not only on the chemical composition and morphology, but also on the type of permeant and the temperature of the atmosphere.

The WVP values of virgin PLA and PLA/alginate bio-composite films are presented in Table 4. As shown, PLA films exhibit lower WVP values (1.44×10^{-6} , g.m/Pa.h.m²), compared with alginate films (15.75×10^{-6} , g.m/Pa.h.m²). This can be attributed to the difference in molecular structure between PLA and sodium alginate. Alginate is more hydrophilic, because of the substituted

hydrophilic group $-\text{COO}-\text{Na}^+$ for alginate.^{36,37} The incorporation of polysaccharides produces an increase in water vapor permeability values. It is worth noting that the WVP value of the PLA/alginate films at 5, 10 and 20% loading is 4.87×10^{-6} , 5.33×10^{-6} and 6.35×10^{-6} , respectively. Adding alginate to the PLA matrix leads to interaction between PLA and alginate, which disrupts the hydrogen bonding network. In addition, the affinity of the blend films for water molecules is stronger than that of the PLA films, as alginate is more hygroscopic compared with PLA.³⁸

Antibacterial activity

We used the antibiotic susceptibility test method based on diffusion from a solid disc to highlight the antibacterial activity of our films against gram-negative bacteria (*Pseudomonas*) and gram-positive bacteria (*Staphylococcus aureus*) after 24 hours of incubation at an adequate temperature of 37 °C. Figures 8 and 9 show the effect of our different films on the two bacteria tested. Based on the digital photos presented in Figures 8 and 9, we note that no activity has been detected in our products against the two bacterial strains used. A positive test must be illustrated by light halos all around the tested product, while dark areas show a phenomenon of bacterial stimulation. Our products do not show any of these two effects and therefore cannot serve as candidates for bacterial inhibition.

However, different materials do not stimulate the growth of bacteria in the same way. Cowan *et al.*³⁹ explains that films without free hydroxyl groups have more antimicrobial activity than those with free hydroxyl groups, leading to an increase in their chemical affinity for membrane lipids. In fact, this sensitivity is in relation with the number of free hydroxyls, of which we can see that the least hydroxylated films are the most active ones.

Previous studies have shown the inhibitory effect of alginate against *Staphylococcus aureus* and *E. coli* bacteria. The strain used in our study is a strain of *Staphylococcus aureus*, a highly pathogenic and very virulent variety. Magallanes *et al.*⁴⁰ found that a methanolic extract from brown seaweed of the *Halopteris scoparia* and *Dictyopteris polypodioides* species is inactive against *Pseudomonas*. Several factors may be responsible for this lack of activity. According to previous studies,^{41,42} some authors believe that these factors are related to the types and nature of

the bioactive substances produced, to the intraspecific variability in the production of secondary metabolites due to seasonal variations,

to extraction protocols and solvents, and to the difference in the methods used to evaluate antibacterial activity.

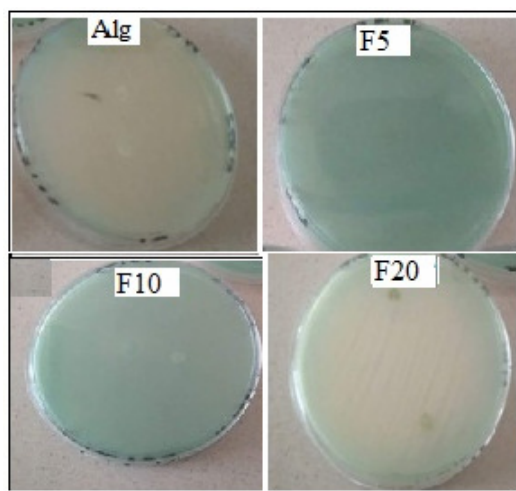


Figure 8: Effect of PLA/alginate films on *Pseudomonas* bacteria

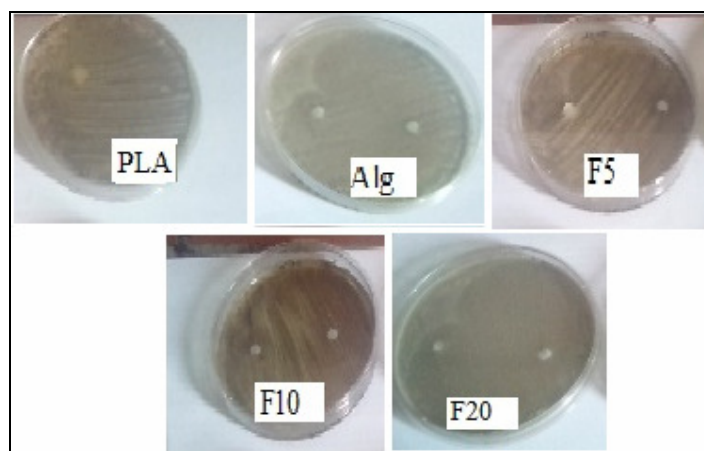


Figure 9: Effect of PLA/alginate films on *Staphylococcus aureus* bacteria

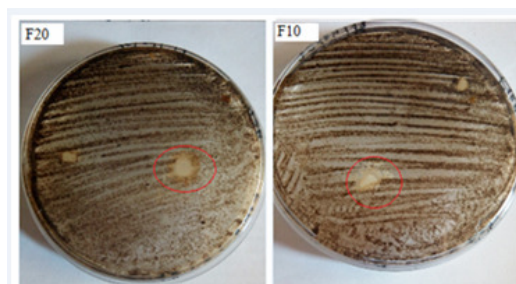


Figure 10: Effect of PLA/alginate films on *Penicillium* fungus

Antifungal activity

The films developed in the present study were also tested against two types of fungi: *Penicillium*

and *Botrytis* after 48 hours of incubation at an adequate temperature of 40 °C.

With regard to the *Botrytis* fungus, the study shows that all the films are inactive, but the F10 and F20 films have an inhibitory effect against the *Penicillium* fungus (Fig. 10). This inhibition is probably due to the active substances present in the alginate, namely proteins, lipids and polyphenols, which are extremely active against this fungus.⁴³ Studies have shown that brown seaweed extracts induce marked inhibition of certain fungi, such as *Penicillium* and *Aspergillus fumigatus*. A chromatographic analysis has revealed that these extracts contain terpene substances, which are responsible for the inhibitory activity obtained.⁴⁴

CONCLUSION

The alginate content of the species *Dictyopteris polypodioides*, estimated at 30%, is very promising and close to those of some alginophytes investigated in the literature, such as *Laminaria digitata* (22-36% PS), the most commonly studied species. The molar masses of alginates extracted from marine algae generally range from about 50000 g/mol to 200000 g/mol. We can see that the molecular weight of our alginate sample falls within this range, with a value of 117931.48 g/mol. The FTIR spectroscopic analysis of the isolated sodium alginate confirms the high uronic acid content of the polysaccharide and the presence of α -L-guluronic acid residues, which indicated that the extraction has been successful. The amorphous state of sodium alginate was confirmed by XRD analysis.

As for the PLA/alginate films, we have drawn the following conclusions. X-ray diffraction analysis has shown that the PLA used is semi-crystalline, with a crystallinity degree of 44%. The introduction of alginate into the PLA matrix disrupts the crystal lattice due to the interactions established between alginate and PLA. The increase in the alginate content induces an increase in water vapor permeability and an increase in the crystallinity content due to the nucleation effect of this charge. Thermogravimetric analysis clearly shows that thermal degradation has been accelerated by the presence of alginate and that the PLA/alginate films generate more residues. Moreover, we note that no antibacterial activity has been detected in our products against the two bacterial strains tested, namely: *Staphylococcus aureus* and *Pseudomonas*. As for the antifungal activity, the films are inactive against the *Botrytis* fungus, but

those containing 10 and 20% of alginate have an inhibitory effect on the *Penicillium* fungus.

REFERENCES

- ¹ F. Garavand, M. Rouhi, S. Razavi, I. Cacciotti and R. Mohammadi, *Int. J. Biol. Macromol.*, **104**, 687 (2017), <http://dx.doi.org/10.1016/j.ijbiomac.2017.06.093>
- ² W. Wiessner, R. C. Starr and E. Schnepf (Eds.), "Algae, Environment and Human Affairs", Biopress, Bristol, England, pp. 258, 1995, <https://trove.nla.gov.au/work/31810207>
- ³ V. Siracusa, P. Rocculi, S. Romani and M. D. Rosa, *Trends Food. Sci. Technol.*, **19**, 634 (2008), <https://doi.org/10.1016/j.tifs.2008.07.003>
- ⁴ V. K. Dhargalkar and N. Pereira, *Sci. Cult.*, **71**, 60 (2005), <http://drs.nio.org/drs/handle/2264/489>
- ⁵ Food and Agriculture Organization of the United Nations (FAO), Year Book of Fishery and Aquaculture Statistics, (2014), <http://www.fao.org/3/a-i5716t.pdf>
- ⁶ H. P. S. Abdul Khalil, T. K. Lai, Y. Y. Tye, S. Rizal, E. W. N. Chong *et al.*, *Express Polym. Lett.*, **12**, 296 (2018), <https://doi.org/10.3144/expresspolymlett.2018.27>
- ⁷ M. Fertah, A. Belfkira, E. M. Dahmane, M. Taourirte and F. Brouillette, *Arabian J. Chem.*, **10**, S3707 (2017), <https://doi.org/10.1016/j.arabjc.2014.05.003>
- ⁸ S. Madhavan and Abirami, *J. Pharm. Sci. Res.*, **7**, 704 (2015)
- ⁹ J. C. Sun and H. P. Tan, *Materials*, **6**, 1285 (2013), <https://doi.org/10.3390/ma6041285>
- ¹⁰ K. Suzuki, Y. Suzuki, M. Tanihara, K. Ohnishi, T. Hashimoto *et al.*, *J. Biomed. Mater. Res.*, **49**, 528 (2000), [https://doi.org/10.1002/\(SICI\)1097-4636\(20000315\)49:4%3C528::AID-JBM11%3E3.0.CO;2-1](https://doi.org/10.1002/(SICI)1097-4636(20000315)49:4%3C528::AID-JBM11%3E3.0.CO;2-1)
- ¹¹ T. Hashimoto, Y. Suzuki, K. Suzuki, T. Nakashima, M. Tanihara *et al.*, *J. Mater. Sci.-Mater. Med.*, **16**, 503 (2005), <https://doi.org/10.1007/s10856-005-0524>
- ¹² I. Eliaz, E. Weil and B. Wilk, *Complement. Med. Res.*, **14**, 358 (2007), <https://doi.org/10.1159/000109829>
- ¹³ L. Meli, E. T. Jordan, D. S. Clark, R. J. Linhardt and J. S. Dordick, *Biomaterials*, **33**, 9087 (2012), <https://doi.org/10.1016/j.biomaterials.2012.08.065>
- ¹⁴ K. Yi, Z. Fan, J. Tang, A. Chen, J. Shao *et al.*, *Colloids Surface B*, **171**, 233 (2018), <https://doi.org/10.1016/j.colsurfb.2018.07.033>
- ¹⁵ B. Wang, P. Li, Y. J. Xu, Z. M. Jiang, C. H. Dong *et al.*, *Composites B*, **194**, 108038 (2020), <https://doi.org/10.1016/j.compositesb.2020.108038>
- ¹⁶ A. Nordmeier and D. Chidambaram, *Energy*, **165**, 603 (2018), <https://doi.org/10.1016/j.energy.2018.09.137>
- ¹⁷ B. Larsen, D. M. S. A. Salem, M. A. E. Sallam, M. M. Mishrikey and A. I. Beltagy, *Carbohydr. Res.*, **338**,

- 2325 (2003), [https://doi.org/10.1016/S0008-6215\(03\)00378-1](https://doi.org/10.1016/S0008-6215(03)00378-1)
- ¹⁸ M. R. Torres, A. P. Sousa, E. A. Silva Filho, D. F. Melo, J. P. Feitosa *et al.*, *Carbohydr. Res.*, **342**, 2067 (2007), <https://doi.org/10.1016/j.carres.2007.05.022>
- ¹⁹ G. Carturan, R. Campostrini, L. Tognana, S. Boninsegna, R. D. Toso *et al.*, *J. Sol.-Gel. Sci. Technol.*, **37**, 69 (2006), <https://doi.org/10.1007/s10971-005-4205-9>
- ²⁰ I. M. Nygard Vold, A. Kare and B. E. Kristiansen, *Biomacromolecules*, **7**, 2136 (2006), <https://doi.org/10.1021/bm060099>
- ²¹ N. Rhein-Knudsen, M. T. Ale, F. Ajallouei and A. S. Meyer, *Food Hydrocolloid.*, **71**, 236 (2017), <http://dx.doi.org/10.1016/j.foodhyd.2017.05.016>
- ²² P. N. Chandia, B. Matsuhira, E. Mejias and A. Moenne Alginic, *J. Appl. Phycol.*, **16**, 127 (2004), <https://doi.org/10.1023/B:JAPH.0000044778.44193.a8>
- ²³ W. Bouzid, M. Yahia, M. Abdeddaim, M. C. Aberkane and A. Ayachi, *Leban. Sci. J.*, **12**, 51 (2011), <http://lsj.cnrs.edu.lb/wp-content/uploads/2015/12/bouzid.pdf>
- ²⁴ T. A. Fenoradosa, G. Ali, C. Delattre, C. Laroche, E. Petit *et al.*, *J. Appl. Phycol.*, **22**, 131 (2009), <http://doi.org/10.1007/s10811-009-9432-y>
- ²⁵ R. M. Silverstein, F. X. Webster and D. J. Kiemle, "Spectrometric Identification of Organic Compounds", 7th ed., John Wiley Inc., 2005
- ²⁶ M. Mathlouthi and J. L. Koenig, *Adv. Carbohydr. Chem. Biochem.*, **44**, 7 (1987), [https://doi.org/10.1016/S0065-2318\(08\)60077-3](https://doi.org/10.1016/S0065-2318(08)60077-3)
- ²⁷ V. Pascalau, V. Popescu, G. L. Popescu, M. C. Dudescu, G. Borodi *et al.*, *J. Alloy. Compd.*, **536**, 418 (2012), <http://doi.org/10.1016/j.jallcom.2011.12.026>
- ²⁸ M. Matet, M. C. Heuzey, E. Pollet, A. Aji and L. Averous, *Carbohydr. Polym.*, **95**, 241 (2013), <https://doi.org/10.1016/j.carbpol.2013.02.052>
- ²⁹ Z. Belattmania, R. Zrid, A. Reani, S. Elatouani, E. M. Sabbar *et al.*, *J. Mater. Environ. Sci.*, **6**, 1654 (2015), https://www.jmaterenvirosci.com/Document/vol6/vol6_N6/193-JMES-1573-2015-Belattmania.pdf
- ³⁰ M. Mihai, M. A. Huneault, B. D. Favis and H. Li, *Macromol. Biosci.*, **7**, 907 (2007), <https://doi.org/10.1002/mabi.200700080>
- ³¹ R. Nasrin, S. Biswas, T. U. Rashid, S. Afrin, R. A. Jahan *et al.*, *Bioactive Mater.*, **2**, 199 (2017), <https://doi.org/10.1016/j.bioactmat.2017.09.003>
- ³² H. E. Salama, M. S. Abdel Aziz and M. W. Sabaa, *Int. J. Biol. Macromol.*, **116**, 443 (2018), <https://doi.org/10.1016/j.ijbiomac.2018.04.183>
- ³³ X. Tang and S. Alavi, *Carbohydr. Polym.*, **85**, 7 (2011), <https://doi.org/10.1016/j.carbpol.2011.01.030>
- ³⁴ Y. Liu, C. J. Zhang, J. C. Zhao, Y. Guo and P. Zhu, *Carbohydr. Polym.*, **139**, 106 (2016), <https://doi.org/10.1016/j.carbpol.2015.12.044>
- ³⁵ F. Xie, E. Pollet, P. J. Halley and L. Avérous, *Prog. Polym. Sci.*, **38**, 1590 (2013), <https://doi.org/10.1016/j.progpolymsci.2013.05.002>
- ³⁶ S. Singh, K. K. Gaikwad and Y. S. Lee, *Int. J. Biol. Macromol.*, **107**, 1879 (2018), <https://doi.org/10.1016/j.ijbiomac.2017.10.057>
- ³⁷ M. J. Fabra, P. Talens and A. Chirlat, *Carbohydr. Polym.*, **74**, 419 (2008), <https://doi.org/10.1016/j.carbpol.2008.03.010>
- ³⁸ Q. Xiao, K. Lu, Q. Tong and C. Liu, *J. Food Process Eng.*, **38**, 155 (2015), <https://doi.org/10.1111/jfpe.12151>
- ³⁹ M. M. Cowan, *Clin. Microbiol. Rev.*, **12**, 564 (1999), <http://cmr.asm.org/>
- ⁴⁰ C. Magallanes, C. Córdova and R. Orozco, *Rev. Peru. Biol.*, **10**, 125 (2003), <http://sisbib.unmsm.edu.pe/BVRevistas/biologia/biologiaNEW.htm>
- ⁴¹ K. Manivannan, G. Thirumaran, G. Karthikai Devi, P. Anantharaman and T. Balasubramanian, *J. Sci. Res.*, **4**, 72 (2009)
- ⁴² P. Rajasulochana, R. Dhamotharan, P. Krishnamoorthy and S. Murugesan, *J. Am. Sci.*, **5**, 20 (2009), <http://doi.org/10.7537/marsjas050309.03>
- ⁴³ L. J. Reichelt and A. M. Borowitzka, *Hydrobiologia*, **116**, 158 (1984), <https://doi.org/10.1007/BF00027657>
- ⁴⁴ J. Moreau, D. Pesando and B. Caram, *Hydrobiologia*, **116**, 521 (1984), <https://doi.org/10.1007/BF00027737>